A Frequency Reconfigurable Rotatable Antenna Design for Cognitive Radio Systems

G. Prema
Professor, Mepco Schlenk Engineering College,

P. Gayatri
Post Graduate Student, Mepco Schlenk Engineering College,

Abstract

Cognitive radio is an emerging technology for efficient use of radio spectrum where the spectrum can be used by the unlicensed secondary users without interference with the licensed primary users. This paper presents a modification of an existing cognitive antenna design: one is a sensing antenna that covers the band from 2-10 GHz and the other is a rotatable frequency reconfigurable antenna which tunes its operating frequency to the corresponding frequency determined by the sensing antenna. The reconfigurable antenna consists of five different antenna patches on the same circular substrate. The frequency agility is achieved by rotating the antenna patch. The rotational motion is brought about by the stepper motor attached at the back of the circular substrate. The two antennas are fabricated on the same substrate and fed at the opposite edges of the substrate. The advantage of this antenna is that there is no need of bias lines as in the case of RF-MEMS, pin-diodes or lumped elements. The comparison between various methods of achieving frequency reconfigurability is presented. The antenna is designed along with the stepper motor and the simulation results obtained in HFSSv11 is provided.

1. Introduction

The radio spectrum is a scarce natural resource. Without spectrum, no wireless telecommunications or wireless internet services would be possible. A cognitive radio is aimed at Dynamic Spectrum Sharing (DSS) [1] and maximum spectrum utilization. A cognitive radio senses the RF environment for detection of RF activity across multiple bands, standards and channels, followed by classification of detected signals. Based on observations and past experience the RF cognitive device determines which possible actions from its current state is optimal and decides on its course of action [2].

One of the major challenges in a cognitive radio RF front end design is the design of reconfigurable antenna. A reconfigurable antenna is essential to sense the entire spectrum of interest and to minimize interference and multipath problems within several frequency bands. Some of the recent works have been implemented using PIN diodes, RF-MEMS or laser diodes [3-5]. For example, in [3] a wideband and a narrowband antenna are placed next to one another and connected via a shorting pin. The wideband antenna is a continuous planar waveguide (CPW)-fed printed hour-glass-shaped monopole antenna that operates from 3 to 11 GHz. The narrow band antenna is a microstrip patch is printed on the reverse side of the substrate and it operates from 5.15 GHz to 5.35 GHz. A reconfigurable C-slot microstrip patch antenna is proposed in [4]. The antenna can operate in dual band or in a very wideband mode. The reconfigurability is achieved by switching on and off the two patches using PIN diodes. A quad-antenna with a directional radiation pattern is presented in [5] whose operating frequency is adjusted by the using radio frequency microelectromechanical system (MEMS) switch. An optically controlled frequency reconfigurable microstrip antenna was implemented in [6] where the slot length is varied to produce a different resonant frequency and narrowband reconfigurability is achieved by integrating laser diodes within the antenna structure to excite the photoconductive switches. In [7], planar arrays of electrically small metallic patches are connected by the field-effect-transistor (FET)-based electronic switches that are used with optical control. Using four PIN diodes, a reconfigurable printed dipole antenna was developed to deliver three operating bands between 5.2 and 5.8 GHz [8]. In [9], a three-dimensional fractal tree structure used RF-MEMS switches to deliver operation over multiple frequency bands. However these antennas (antennas using RF-MEMs and PIN-diode switches) need simultaneous fabrication of the antenna and switches on the substrate to mitigate the effects of package parasitic and other non-linear effects that would be created if

the switches were pre-packaged and attached using solder or bondwires.

Some research has also been made on the mechanical/structural changes to produce frequency reconfigurability. In [10], there are two antennas incorporated on the same substrate. The first antenna is an ultra wideband (UWB) antenna covering the spectrum from 3.1-11 GHz for channel sensing. It is a slotted polygonal patch. The second antenna is a frequency reconfigurable rotational patches printed on the circular substrate. The patches are rotated by 180^{o} and each time a different triangular patch is fed. They cover the bands from 5.3-9.15 GHz and 3.4-4.85 GHz. However, the coverage band of the reconfigurable antenna is small. In [11], continuous frequency changes is enabled by mechanical changes in a magnetically actuated microstrip antenna where a patch is positioned at an angle over the substrate. Small changes in the angle changes the operating frequency.

This design is not a new one, it is a modification of an existing one [12] to get and fabricate a more efficient antenna. The antenna structure incorporates both a sensing antenna and reconfigurable antenna onto the same substrate. The sensing antenna covers the band from 2 - 10 GHz, while the reconfigurable antenna is able to tune its operating frequency through the entire band covered by the sensing antenna. Reconfigurability is achieved by feeding different antenna patches at different instances. This frequency reconfigurability is achieved by rotational motion. In Section 2, the comparison between the rotatable reconfigurable antenna and the RF MEMS/PIN-diode-based reconfigurable antenna is presented. In Section-3, the architecture of the investigated cognitive antenna structure is shown. The numerical simulations of the RF performance are shown in Section-4. Section-5 has the future work and conclusion.

2. Comparison between Rotatable Reconfigurable Antenna, RF MEMS/PIN-diode-based and Optically Reconfigurable Antenna Systems

In this design, the rotatable reconfigurable antenna has the advantage that there is no need of bias lines which affects the radiation characteristics of the antenna. RF-MEMS/PIN diode-based reconfigurable antenna systems require the use of bias lines. It also requires the bias lines to lie on the same plane as that of the antenna. In Optically Pumped Reconfigurable Antenna ("OPRAS") [6], photoconductive switches are used and laser diodes are integrated to the antenna structure and there is no need of bias lines to be on the same plane as the antenna.

Ταβλε 1 shows the comparison between various switching techniques available [13-15] in terms of voltage/current requirements, switching speed and power consumption. Power consumption is more for RF-MEMS and PIN-diodes. Like RF-MEMS/PIN diode-based antennas, the optically pumped reconfigurable antennas also need some power to activate the switching elements and the power consumption is in between RF-MEMS and PIN-diodes. Optically controlled reconfigurable antenna needs a higher level of driving voltage but performs faster than the other two methods. Rotatable antennas sequentially sense the spectrum. The sensing and processing duration determine its performance. The sensing speed can be increased by increasing the speed of the stepper motor. But the speed of the stepper motor has to be optimum so that the antenna does not miss any changes in the surrounding RF environment.

Ταβλε 1. Χομπαρισον βετωεεν ωαριουσ φρεθυενχψ ρεχονφιγυραβλε τεχηνιθυεσ

	"OPRAS"	RF-MEMS	PIN-diodes
Voltage(V)	1.8-1.9	20-100	3-5
Current(mA)	0-87	0	3-20
Switching time	3-9 (μs)	1-200 (μs)	1-100 (ns)
Power Consumption (mW)	0-50	0.05-0.1	5-100

The RF-MEMS based antennas have poor reliability [16]. In PIN-diodes, the stored charge is insufficient to control the RF current and it exhibits a non-linear behavior at RF frequencies [17]. There is also intermodulation distortion and harmonics in PIN-diodes which makes it less reliable for cognitive radio applications. Integration problems occur with both RF-MEMS and PIN diodes and such problems are comparatively less with photoconductive switches and there are no such problems in rotatable antennas. Another advantage of the rotatable reconfigurable antenna is that there are no intermodulation distortion and spurious harmonics as in the case of the PIN diodes.

3. Antenna Structure

The antenna structure consists of an ultra wideband (UWB) and a reconfigurable narrowband antenna placed next to each other. The antenna top view is shown in Φιγ. 1(α); its bottom view is shown in Φιγ. 1(β). The left module is the reconfigurable antenna while the right module is the sensing antenna. The antenna is printed on a 70 mm × 50 mm Rogers Duroid 5880 substrate with dielectric constant 2.2 and

height 1.6 mm. The simulations were done in HFSSv11.

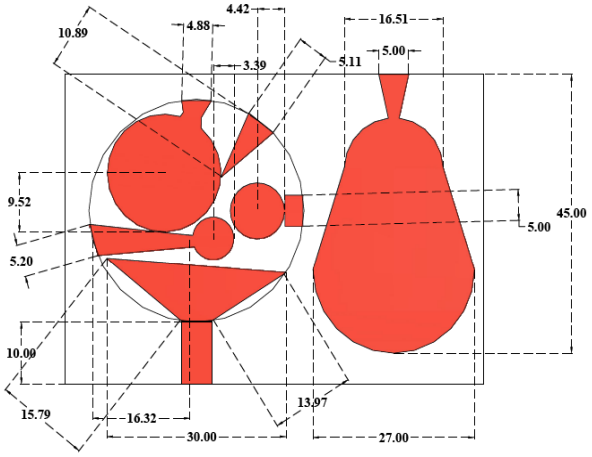

(α)

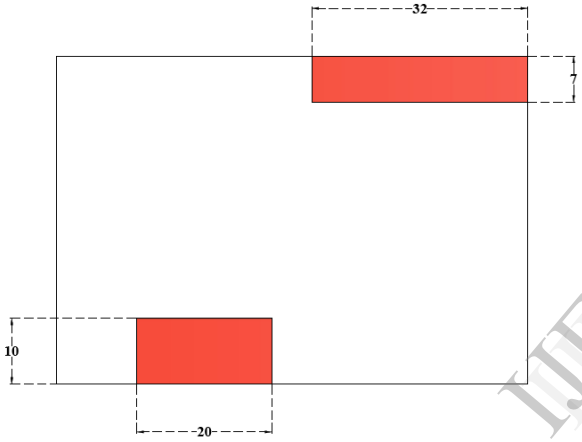

(β)

Φιγ.1. Αντεννα Στρυχτυρε. (α)Τοπ σιεω. (β)Βοττομ σιεω.

3.1. Sensing antenna

The sensing antenna is a modified egg-shaped printed monopole antenna which is fed via a tapered stripline. It has a major axis of 38 mm (≈ 0.25 * λ_l) and a minor axis of 27 mm (≈ .18 * λ_l) where λ_l is the wavelength at lower frequency (2 GHz). The tapered stripline takes care of all the impedance transformations at different frequencies. The tapering follows an exponential pattern. The sensing antenna has partial ground dimensions of 32 mm × 7 mm which makes it to act like a vertical antenna. The antenna radiation pattern at $\Phi=0^0$ and $\Phi=90^0$ at Position-1 for f=7.12 GHz and 9.6125 GHz is as shown in the Φιγ 2(α) and Fig 2(b) sequentially. The radiation pattern is omni-directional due to the fact that the antenna has partial ground and is able to radiate above and below the substrate. The 3D Radiation plot at Position-1 for f=7.12 GHz is as shown in the Φιγ 3.

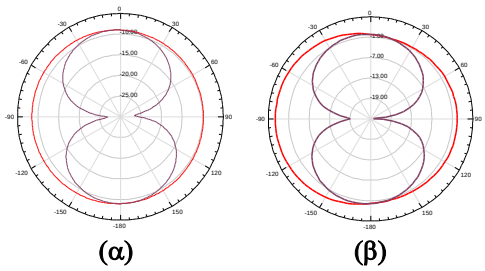

(α) (β)

Φιγ. 2. Ραδιατιον Παττερν οφ Σενσινγ αντεννα ατ $\Phi=0^0$ ανδ $\Phi=90^0$
(α) Ατ 7.12 ΓΗζ (β) Ατ 9.6175 ΓΗζ

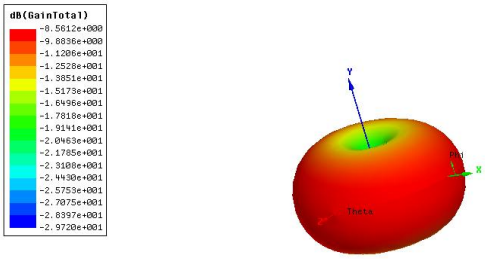

Φιγ. 3. 3Δ σισυαλιζατιον παττερν οφ Σενσινγ αντεννα ατ 7.12 ΓΗζ

3.2. Communicating antenna

The antenna consists of five different patches that are printed on a circular substrate of radius 18 mm. The patches are fed via a microstrip feed line of dimensions 10 mm × 5.05 mm. Each patch is designed to operate in a particular frequency band. The shape and the position of the antenna patches are optimized using parametric analysis in HFSSv11.The frequency tuning is achieved by physically altering the patch shape. At each rotation stage, a different patch is excited and a different resonant frequency is achieved, each at one of the sensing antenna results. This is the aim of the reconfigurable process. The circular substrate is rotated via a stepper motor attached at the back. The stepper motor characteristic is extracted from [18]. The stepper motor is modeled in HFSS to account for its effect. The rotating part of the stepper motor is a cylinder of length 10 mm and diameter 10 mm.

4. Simulation Results

The modification of the existing design is in the dimensions of the patches such that we can make the cognitive radio to work at the sensing antenna results otherwise the cognitive radio would work in wideband. The frequency reconfigurability is achieved

by making mechanical changes in the antenna arrangement as shown in Φιγ 4. Shape-1 excitation of reconfigurable antenna corresponds to Position-1, Shape-2 excitation corresponds to Position-2, Shape-3 is excited at Position-3, similarly Shape-4 is excited at Position-4 and Position-5 is when Shape-5 is excited.
The side view of the antenna along with the stepper motor in HFSS is as shown in Φιγ. 5(α). and the front view with reconfigurable antenna in Position-1 is as shown in Φιγ. 5(β).

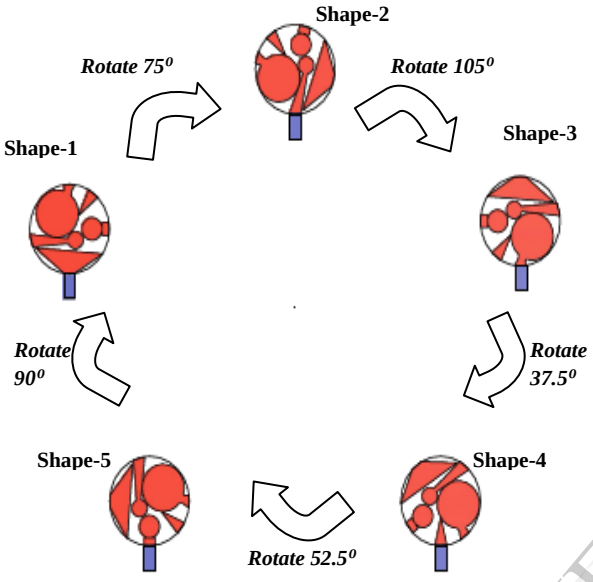

Φιγ. 4. Φρεθυενχψ ρεχονφιγυραβιλιτψ προχεσσ.

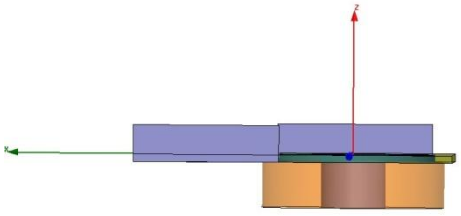

(α)

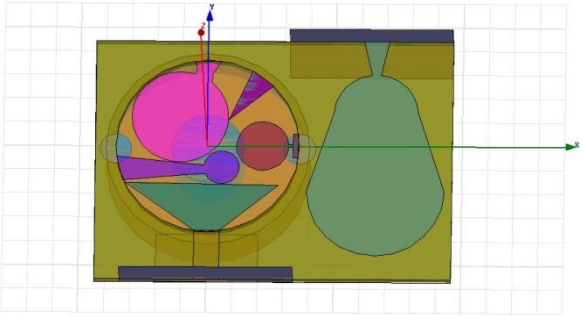

(β)

Φιγ. 5. Αντεννα ωιεω ιν ΗΦΣΣ (α) Σιδε ςιεω. (β) Φροντ ωιεω ωτη ρεχονφιγυραβλε αντεννα ιν Ποσιτιον–1.

4.1. Position-1

The sensing antenna return loss at Position-1 is shown in Φιγ. 6(α) and the reconfigurable antenna at Position-1 with Shape-1 excited is shown in Φιγ 6(β). The sensing antenna at Position-1 shows excitation for five bands, 2.1925 GHz, 3.7225 GHz, 4.42 GHz, 5.5225 GHz, 7.12 GHz, 9.6175 GHz, which exceed -10 dB return loss. Shape-1 of reconfigurable antenna covers a band from 4.2 GHz to 6 GHz and has a resonance at 5.545 GHz, which is near one of the resonance frequencies, 5.5225 GHz, of the sensing antenna. The return loss is -30.9124 dB at 5.545 GHz. The antenna is rotated by 75⁰ to get Shape-2.

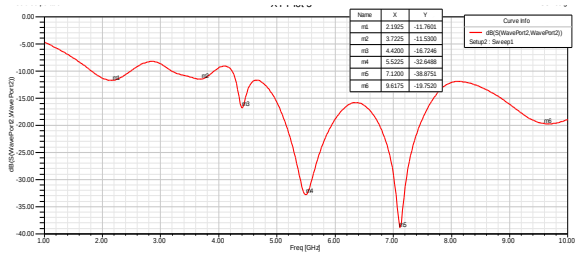

(α)

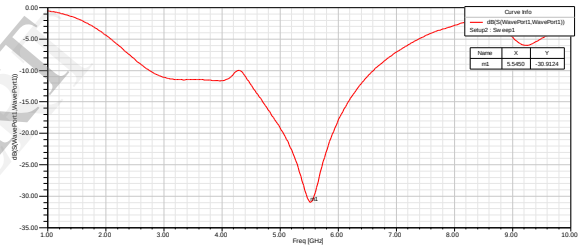

(b)

Φιγ. 6. Ρετυρν λοσσ πλοτσ ατ Ποσιτιον–1. (α) Σενσινγ αντεννα. (β) Σηαπε–1.

4.2. At Position-2

The sensing antenna return loss at Position-2 is shown in Φιγ 7(α) and the reconfigurable antenna at Position-2 is shown in Φιγ 7(β). The sensing antenna at Position-2 shows excitation for two bands, 7.345 GHz, 9 GHz, which exceed -10 dB return loss. Shape-2 of reconfigurable antenna covers a band from 6.6 GHz to 10 GHz tuning at 7.615 GHz, which is very near to one of the operating frequency of sensing antenna, 7.345 GHz. The return loss of the antenna is -54.135 dB at 7.615 GHz. The antenna is rotated by 105⁰ to get Shape-3.

4.3. At Position-3

The sensing antenna return loss at Position-3 is shown in Φιγ 8(α) and the reconfigurable antenna at Position-3 is shown in Φιγ 8(β). The sensing antenna at Position-3 shows excitation at four bands 5.5675 GHz,

7.075 GHz, 3.52 GHz, 2.1475 GHz, which exceed -10 dB. Shape-3 covers a band from 2 GHz to 3.3 GHz and has a resonance at 2.17 GHz which is very near to one of the resonance frequencies, 2.1475 GHz, of the sensing antenna. The return loss of the antenna is -20.1067 dB at 2.17 GHz. The antenna is rotated by 37.5^0 to get Shape-4.

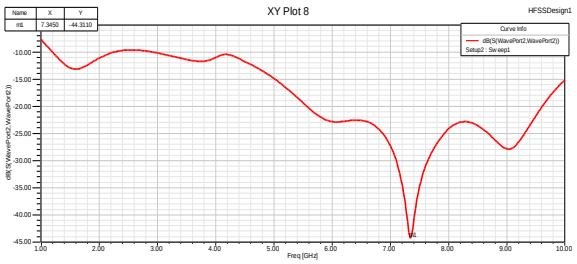

(α)

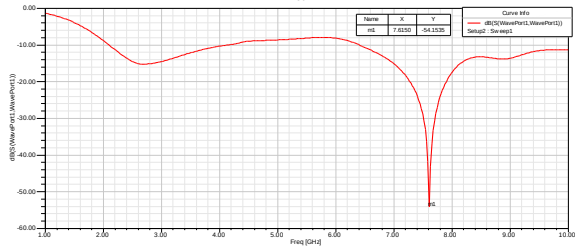

(b)

Φιγ. 7. Ρετυρν λοσσ πλοτσ ατ Ποσιτιον–2.
(α) Σενσινγ αντεννα. (β) Σηαπε–2.

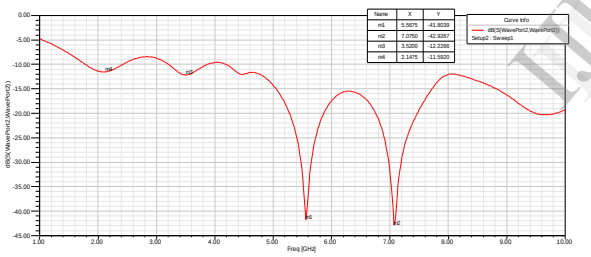

(α)

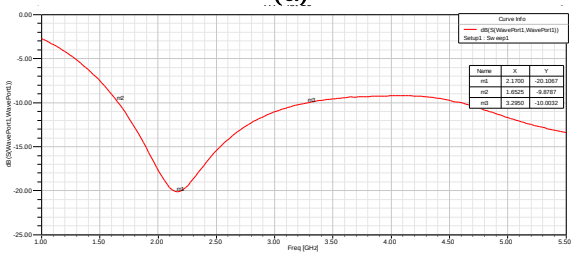

(b)

Φιγ. 8. Ρετυρν λοσσ πλοτσ ατ Ποσιτιον–3.
(α) Σενσινγ αντεννα. (β) Σηαπε–3.

4.4. At Position-4

The sensing antenna return loss at Position-4 is shown in Φιγ 9(α) and the reconfigurable antenna at Position-4 is shown in Φιγ 9(β). The sensing antenna, at Position-4 shows excitation at three bands 3.7675 GHz, 7.12 GHz, 9.2126 GHz which exceed -10 dB. Shape-4 covers a band from 5.6 GHz to 6.9 GHz and has a resonance at 6.4775 GHz, which is near to the resonance frequency 7.12 GHz of the sensing antenna. The return loss of the antenna is -50.7317 at 6.4775 GHz. The antenna is rotated by 52.5^0 to get Shape-5.

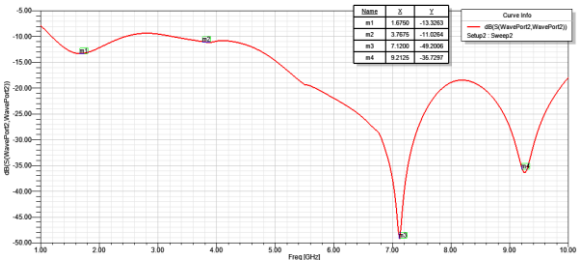

(α)

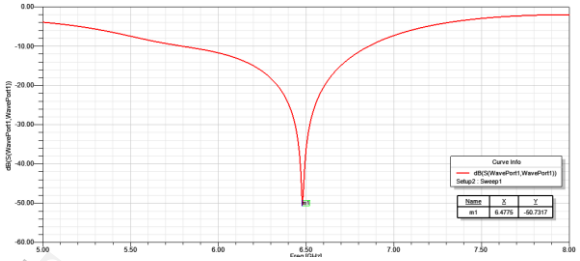

(β)

Φιγ. 9. Ρετυρν λοσσ πλοτσ ατ Ποσιτιον–4.
(α) Σενσινγ αντεννα. (β) Σηαπε–4.

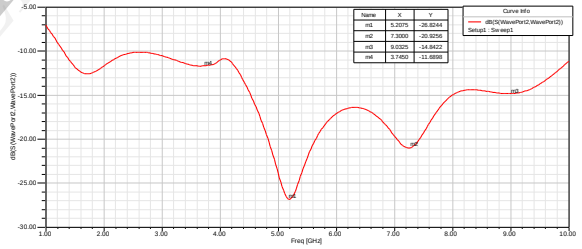

(α)

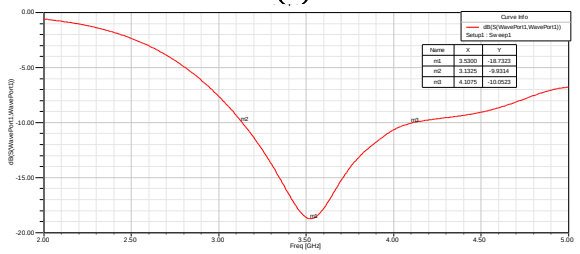

(β)

Φιγ. 10. Ρετυρν λοσσ πλοτσ ατ Ποσιτιον–5.
(α) Σενσινγ αντεννα. (β) Σηαπε–5.

4.5. At Position-5

The sensing antenna return loss at Position-5 is shown in Φιγ 10(α) and the reconfigurable antenna at Position-5 is shown in Φιγ 10(β). The sensing antenna at Position-5 shows excitation at four bands 5.2075

GHz, 7.3 GHz, 9.0325 GHz, 3.745 GHz. Shape-5 covers a band from 3.1 GHz to 4.1 GHz and has resonance at 3.1325 GHz, which is very near to the resonance frequency 3.745 GHz of the sensing antenna. The return loss of the antenna is -18.7323 dB at 3.1325 GHz. The antenna is rotated by 90^{o} to get Shape-1.

4.6. Frequency Reconfigurability

The frequency reconfigurability of the antenna can be noted from the return loss results shown in Φιγ 11. The Radiation pattern of the reconfigurable antenna at XZ plane ($\Phi=0^{o}$) is presented in Φιγ. 12. The antenna has the property to tune on 4.2 – 6 GHz with resonance at 5.545 GHz (Position-1), 6.4 – 10 GHz with resonance at 7.615 GHz (Position-2), 2 – 3.3 GHz with resonance at 2.17 GHz (Position-3), 5.8 – 6.6 GHz with resonance at 6.4775 GHz (Position-4) and 3.1 – 4.1 GHz with resonance at 3.1325 GHz (Position-5). For all the positions the antenna shows omni-directional radiation pattern and hence it preserves the radiation characteristics.

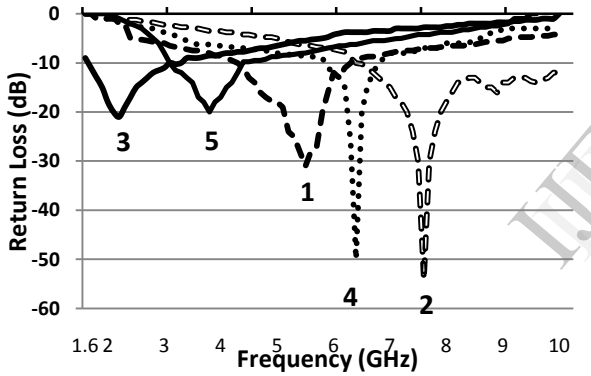

Φιγ 11. Συπεριμποσεδ Ρετυρν λοσσ πλοτσ οφ ρεχονφιγυραβλε αντεννα σεχτιονσ

Ταβλε 2. Συμμαρψ οφ ρεχονφιγυραβλε αντεννα ρεσυλτσ

	Bandwidth (GHz)	Operating Frequency (GHz)	Return Loss (dB)	Peak Gain (dB)
Shape-1	(4.2-6)	5.545	-30.912	5.16
Shape-2	(6.4-10)	7.615	-54.135	6.70
Shape-3	(2-3.3)	2.17	-20.106	4.74
Shape-4	(5.8-6.6)	6.4775	-50.731	6.89
Shape-5	(3.1-4.1)	3.1325	-18.732	5.08

Ταβλε 2 shows the reconfigurable antenna results for each patch shape. Table 3 shows the summary of the sensing antenna results at various positions of the reconfigurable antenna. From Ταβλε–2 we can infer that the five patches collectively cover the operating band of the sensing antenna.

Also, by comparing the communicating antenna results from Ταβλε 2 and the sensing antenna results from Ταβλε 3, it can be seen that the communicating antenna operates at exactly one of the sensing antenna results thereby making the cognitive radio to operate in narrowband. Shape-1 of reconfigurable antenna has a resonance at 5.545 GHz, which is near one of the resonance frequencies, 5.5225 GHz, of the sensing antenna at Position-1. Shape-2 resonates at 7.615 GHz, which is very near to one of the operating frequency, 7.345 GHz, of sensing antenna at Position-2. Shape-3 has a resonance at 2.17 GHz which is very near to one of the resonance frequencies, 2.1475 GHz, of the sensing antenna at Position-3. Shape-4 has a resonance at 6.4775 GHz, which is near to the resonance frequency 7.12 GHz of the sensing antenna at Position-4. Shape-5 has resonance at 3.1325 GHz, which is very near to the resonance frequency 3.745 GHz of the sensing antenna at Position-5.

Ταβλε 3. Συμμαρψ οφ Σενσινγ αντεννα ρεσυλτσ

Bandwidth (GHz)	Operating Frequency (GHz)	Return Loss (dB)	Gain (dB)
Position-1			
(2-2.5)	2.1925	-11.7601	4.86
(3.1-4.2)	3.7225	-11.53	5.60
(4.2-4.6)	4.42	-16.7246	4.84
(4.6-6.4)	5.5225	-32.6488	5.20
(6.4-8.2)	7.12	-38.8751	6.15
(8.2-10)	9.6175	-19.752	4.98
Position-2			
(6.6-8.4)	7.345	-44.31	6.25
(8.4-10)	9	-28	5.20
Position-3			
(2-2.8)	2.1475	-11.592	4.66
(3-4)	3.52	-12.2266	5.82
(4.6-6.4)	5.5675	-41.8039	5.25
(6.4-8)	7.075	-42.9267	6.74
Position-4			
(3.4-4)	3.7675	-11.0264	3.84
(5.4-8.2)	7.12	-49.2006	4.52
(8.2-10)	9.2126	-35.7297	5.06
Position-5			
(3-4.2)	3.745	-11.6898	3.88
(4.2-6.2)	5.2075	-25.8244	4.21
(6.2-8)	7.3	-20.9256	4.53
(8-10)	9.0325	-14.8422	4.87

4.7. Coupling

When two antennas are fabricated on the same substrate, coupling ($|S_{21}|^2$) between the two antennas is important to be determined. The simulated coupling at various positions is as shown in the Φιγ 13. The coupling between the sensing antenna and the reconfigurable antenna are found to be below -20 dB in the operating range at various reconfigurable section positions since the antennas are fed at the opposite edges of the substrate. The space requirement of the antenna is reduced by fabricating the two antennas on the same substrate.

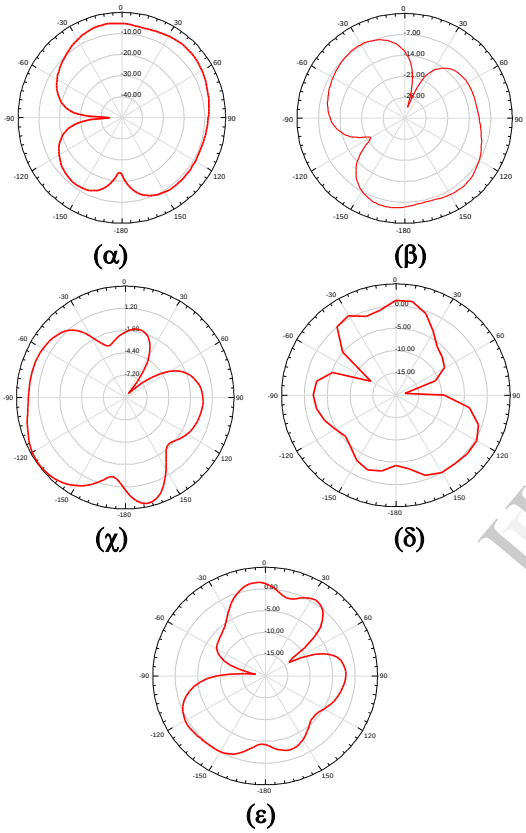

(α) (β) (χ) (δ) (ε)

Φιγ. 12. Ραδιατιον Παττερν οφ ρεχονφιγυραβλε αντεννα ατ ΞΖ πλανε(Φ=0⁰).
(α) Σηαπε–1 ατ 5.545 ΓΗζ. (β) Σηαπε–2 ατ 7.615 ΓΗζ. (χ) Σηαπε–3 ατ 2.17 ΓΗζ. (δ) Σηαπε–4 ατ 4.4775 ΓΗζ. (ε) Σηαπε–5 ατ 3.1325 ΓΗζ.

This antenna can be used in energy detection technique of spectrum sensing where the spectrum of interest can be divided into sub-bands and it can reduce the need for high resolution ADCs [19] to sample at a higher rate. For example in [20], an ADC was developed to sample at a rate of 16 GS/s but only with 6-bit resolution. Trade-off exists between the sampling rate and resolution which can be optimized further if the obtained centre frequencies from the antennas are converted to IF range (MHz range).

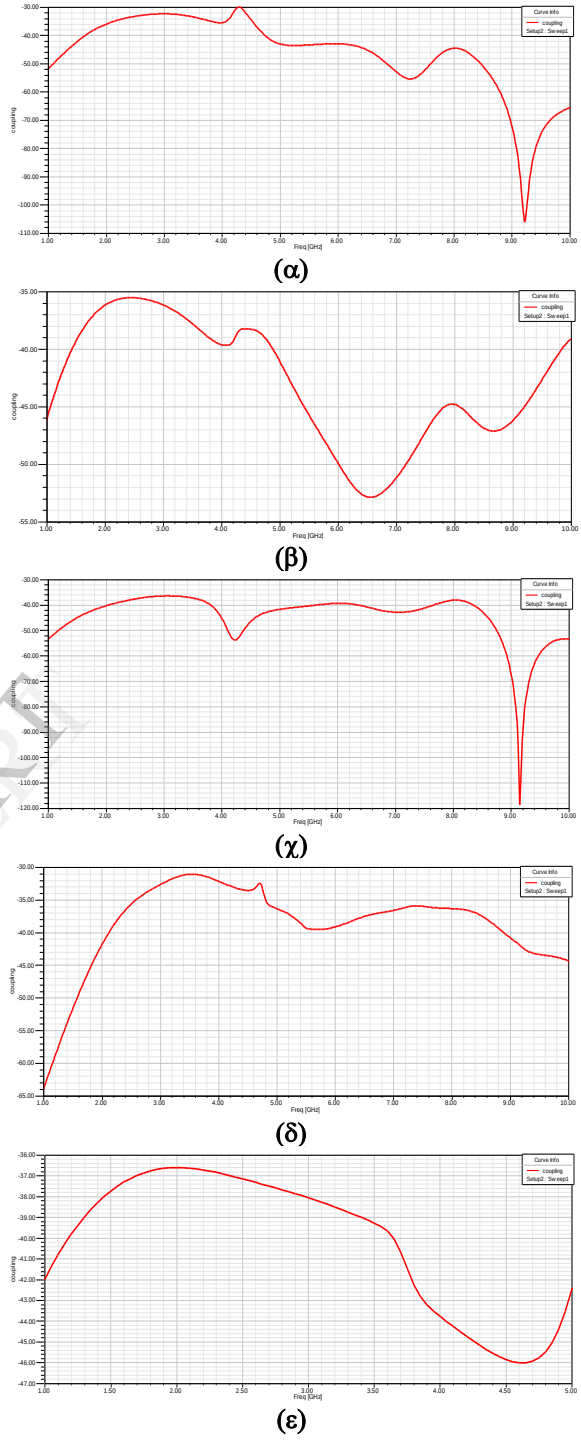

(α) (β) (χ) (δ) (ε)

Φιγ. 13. Χουπλινγ βετωεεν τηε σενσινγ αντεννα α νδ τηε ρεχονφιγυραβλε αντεννα. (α) Ατ Ποσιτιον –1. (β) Ατ Ποσιτιον–2. (χ) Ατ Ποσιτιον–3. (δ) Ατ Ποσιτιον–4. (ε) Ατ Ποσιτιον–5.

5. Conclusion

In this design, no bias lines are needed to activate the switches. This allows for easier integration of the antenna in a complete RF chain and reduces the amount of complexity that is introduced by the bias lines. A stepper motor is needed to achieve the required rotation. This design is not new, it is designed and fabricated in another paper but the new modification is done in the reconfigurable structure. We have modified the dimensions of the patches. This modification allows the cognitive radio to work exactly at the bands of sensing results. The reconfigurable antenna we designed selects one of the sensing frequency results. Our design is more accurate than any design that has the same idea. Our future work will be to make use of the antenna for blind energy detection followed by cyclostationary detection, where the disjoint sub-bands obtained from the antenna is sampled with the centre frequencies, f1=5.545 GHz, f2=7.615 GHz, f3=2.17 GHz, f4=6.4775 GHz, f5=3.1325 GHz, converted to MHz range thereby reducing the constraint of using a high resolution ADC to sample the spectrum of interest (2-10 GHz).

References

[1] D'Iitri, S., McHenry. M, "Dynamic spectrum access moves to the forefront." Defence Electronics. April 2008, p. S3–S6.

[2] J. Mitola, "Cognitive radio: An integrated agent architecture for software defined radio," Ph.D. dissertation, Royal Institute of Technology (KTH), Stockholm, Sweden, 2000.

[3] E. Ebrahimi and P. S. Hall, "A dual port wide-narrowband antenna for cognitive radio," in *Proc. 3rd Eur. Conf. Antennas Propag.*,Mar. 2009,pp. 809–812.

[4] H. F. AbuTarboush, S. Khan, R. Nilavalan, H. S. Al-Raweshidy, andD. Budimir, "Reconfigurable wideband patch antenna for cognitive radio," in *Proc. Loughborough Antennas Propag. Conf.*, Nov. 2009, pp. 141–144.

[5] G. T. Wu, R. L. Li, S. Y. Eom, S. S. Myoung, K. Lim, J. Laskar, S. I.Jeon, and M. M. Tentzeris, "Switchable quad-band antennas for cognitive radio base station applications," *IEEE Trans. Antennas Propag.*, vol. 58, no. 5, pp. 1466–1476, May 2010.

[6] Y. Hawk, A. R. Albrecht, S. Hemmady, G. Balakrishnan, and C. G.Christodoulou, "Optically pumped frequency reconfigurable antenna design," *IEEE Antennas Wireless Propag. Lett.*, vol. 9, pp. 280–283, Mar. 2010.

[7] L. N. Pringle, P. H. Harms, S. P. Blalock, G. N. Kiesel, E. J. Kuster, P.G. Friederich, R. J. Prado, J. M. Morris, and G. S. Smith, "A reconfigurable aperture antenna based on switched links between electrically small metallic patches," *IEEE Trans. Antennas Propag.*, vol. 52, no. 6, pp. 1434–1445, Jun. 2004.

[8] Roscoe, D.J., Shafai, L., Ittipiboon, A., Cuhaci, M., and Douville, R., "Tunable dipole antennas," *Proceedings of the IEEE/URSI International Symposium on Antennas and Propagation*, vol. 2, pp. 672–675, 1993.

[9] Petko, J.S., and Werner, D.H., "Miniature reconfigurable three-dimensional fractal tree antennas," *IEEE Transactions on Antennas and Propagation*, vol. 52, pp. 1945–1956, August 2004.

[10] Y. Tawk and C. G. Christodoulou, "A new reconfigurable antenna design for cognitive radio," *IEEE Antennas Wireless Propag. Lett.*, vol. 8, pp. 1378–1381, 2009.

[11] Langer, J.-C., Zou, J., Liu, C., and Bernhard, J.T., "Reconfigurable out-of-plane microstrip patch antenna using MEMS plastic deformation magnetic actuation," *IEEE Microwave and Wireless Components Letters*, vol. 13, pp. 120–122, March 2003.

[12] Y. Tawk, J. Costantine, K. Avery, and C. G. Christodoulou, "Implementation of a cognitive radio front-end using rotatable controlled reconfigurable antennas," *IEEE Trans. Antennas Propag.*, vol. 59, no. 5, pp. 1773–1778, May 2011.

[13] Y. Yashchyshyn, "Reconfigurable antennas by RF switches technology,"in *Proc. 5th Int. Conf. Perspective Technol. Meth. MEMS Design*, Apr. 2009, pp. 155–157.

[14] G. M. Rebeiz, *RF MEMS Theory, Design and Technology*. Hoboken NJ: Wiley, 2003.

[15] Y. Tawk, S. Hemmady, G. Balakrishnan, and C. G. Christodoulou, "Measuring the transition switching speed of a semiconductor-based photoconductive switch using RF techniques," in *Proc. IEEE Int. Symp. Antennas Propag.*, Jul. 2011, pp. 972–975.

[16] Carton, C. G. Christodoulou, C. Dyck, and C. Nordquist, "Investigating the impact of carbon contamination on RF MEMS reliability," in *Proc. IEEE Antennas Propag. Int. Symp.*, Jul. 2006, pp. 193–196.

[17] R. H. Caverly and G. Hiller, "Distortion properties of MESFET and PIN diode microwave switches," in *Proc. IEEE MTT-S Int. Microw. Symp.*, Jun. 1992, vol. 2, pp. 533–536.

[18] [Online]. Available: http://www.digikey.com.

[19] T. Atwood, "RF channel characterization for cognitive radio using support vector machines," Ph.D. dissertation, University of New Mexico, Nov. 2009.

[20] C.-C. Huang, C.-Y. Wang, and J.-T. Wu, "A CMOS 6-bit 16-gs/s time interleaved ADC using digital background calibration techniques," *IEEE J. Solid-State Circuits*, vol. 46, no. 4, pp. 848–858, Apr. 2011.